

## Determination of third-order nonlinear susceptibility $\chi^{(3)}$ through measurements in the picosecond time domain

B. K. Rhee and W. E. Bron

*Department of Physics, Indiana University, Bloomington, Indiana 47405*

J. Kuhl

*Max-Planck-Institut für Festkörperforschung, Heisenbergstrasse 1,  
7000 Stuttgart-80, Federal Republic of Germany*

(Received 14 June 1984)

The temporal dependence, in the picosecond domain, of the coherent anti-Stokes-Raman signal associated with the LO Raman resonance in GaP is used to obtain the complex components of the third-order nonlinear susceptibility  $\chi^{(3)}$ . Under certain experimental conditions the measurements in the temporal domain are markedly advantageous compared with the traditional measurements in the spectral domain.

Determination of the optical-phonon dephasing time  $\Gamma^{-1}$ , and of the third-order nonlinear (nonresonant) electronic susceptibility  $\chi^{(3)}$  have in the past been achieved experimentally through separate measurements in the frequency domain, specifically, through Raman linewidth measurements and through the frequency dependence of the three-wave mixing intensity at a Raman active lattice, molecular, or excitonic resonance.<sup>1</sup> Recently, it has become evident that these parameters can also be obtained through a single measurement of the three-wave mixing signal in the picosecond time (rather than frequency) domain.<sup>2,3</sup> We demonstrate that, in some cases, the temporal technique is markedly advantageous relative to the spectral technique. Moreover, we present the first determination, by these means, of all active components of  $\chi^{(3)}$  for an anisotropic solid; specifically, GaP at room temperature for which we have previously reported  $\Gamma$  and its temperature dependence.<sup>3</sup>

The basic nonlinear system involves the interaction of three incident laser beams to produce a macroscopic polarization of the medium which in turn produces a fourth coherent light beam. If the frequencies of the three incident beams are taken to be, respectively,  $\omega_l$ ,  $\omega_p$ , and  $\omega_s$ , then a fourth beam is found at  $\omega_c = 2\omega_l - \omega_s$ .<sup>4</sup> If in addition,  $\omega_l - \omega_s$  equals some Raman active resonance (at  $\omega_v$ ) in the medium, coherent excitation of the resonant state occurs<sup>1</sup> and the so-called coherent anti-Stokes-Raman scattering (CARS) signal is produced.

The governing expression for the frequency dependence of the CARS signal,  $I(\omega)$ , appears elsewhere.<sup>1</sup> The corresponding expression for the temporal dependence of the CARS signal,  $I(\Delta t)$ , is<sup>2</sup>

$$I(\Delta t) = AS(\Delta k) \int_{-\infty}^{+\infty} dt |\bar{\mathbf{E}}_p(t - \Delta t) [NR_a Q(t) + 3\chi^{(3)} \times \bar{\mathbf{E}}_l(t) \bar{\mathbf{E}}_s^*(t)]|^2, \quad (1)$$

where

$$S(\Delta k) = \sin^2(\Delta kL/2) / (\Delta kL/2)^2 \quad (2)$$

and

$$\Delta \bar{\mathbf{k}} = \bar{\mathbf{k}}_c - (\bar{\mathbf{k}}_l + \bar{\mathbf{k}}_p - \bar{\mathbf{k}}_s) \quad (3)$$

and

$$\dot{Q} + \Gamma \dot{Q} + \omega_v^2 Q = R_a \mu^{-1} \bar{\mathbf{E}}_l(t) \bar{\mathbf{E}}_s^*(t). \quad (4)$$

The subscripts  $l$ ,  $s$ , and  $p$  in Eqs. (1)–(4) refer to the three incident laser fields used to excite ( $l, s$ ) and to probe ( $p$ ) the temporal evolution of the excited resonant state, and  $R_a$  is the Raman tensor.

In the experiment reported here, a mode-locked argon-ion laser is used to synchronously pump two R6G dye lasers to produce picosecond pulse trains with fields  $\bar{\mathbf{E}}_l(\omega_l)$ ,  $\bar{\mathbf{E}}_p(\omega_p = \omega_l)$ , and  $\bar{\mathbf{E}}_s(\omega_s)$ .<sup>5</sup> Coherent excitation of longitudinal optical (LO) phonons is obtained by setting  $\omega_l - \omega_s = \omega_v$ ; here,  $\omega_l = 17350 \text{ cm}^{-1}$  and  $\omega_s = 16947 \text{ cm}^{-1}$ . The coherent amplitude  $Q$  of the excited phonon packet is given by Eq. (4). The wave-vector mismatch of  $I(\Delta t)$  is given by  $\Delta k$ ; it is set experimentally to approximately zero [hence,  $S(\Delta k) \sim 1$ ]. Finally,  $\Delta t$  is the temporal delay between the pulses of the probe laser  $p$  and those of the lasers  $l$  and  $s$ ;  $\mu$  is the reduced lattice mass,  $N$  the number of primitive cells per  $\text{cm}^3$ , and  $A = 2\pi\omega_c^2 L^2 / c\epsilon_c$ . In the expression for  $A$ ,  $c$  is the speed of light,  $L$  the effective length within the medium over which spatial overlap of the three-wave mixing exists, and  $\epsilon_c$  is the dielectric constant of the medium at  $\omega_c$ .

According to Eq. (1),  $I(\Delta t)$  has two components. The two contributions can be clearly seen in Fig. 1 of Ref. 3 which displays a normalized  $I(\Delta t)$  as a function of  $\Delta t$ . If  $\omega_l - \omega_s$  is detuned from the LO phonon frequency  $\omega_v$ ,  $Q$  becomes very small and only that part of Eq. (1) controlled by  $\chi^{(3)}$  remains. Thus, a purely "electronic" part of  $I(\Delta t)$  [ $I_E(\Delta t)$ ], i.e., independent of any Raman excitation, appears under these circumstances and is indicated by the curve with solid circles in the region  $-30 < \Delta t < +20$  ps in Fig. 1 of Ref. 3. If  $\omega_v = \omega_l - \omega_s$ , the curve with crosses appears. The exponentially decreasing part of the signal is controlled by  $\Gamma$  and corresponds to the dephasing of the coherent LO phonon packet referred to earlier.<sup>3</sup>

It follows from Eqs. (1) and (4) that, once  $\Gamma$  is determined, a further analysis of the full  $I(\Delta t)$  becomes possible in terms of the integration over the temporal profiles of the laser fields  $E_i(t)$ , plus an independent evaluation of the Raman tensor elements  $R_a$ . The result of this procedure leads to a determination of the components of  $\chi^{(3)}$ . In the analysis presented here, the actual form of the temporal profiles of the laser pulses are obtained from  $I_E(\Delta t)$  (through which the asymmetry factor  $\delta$  is determined) and from the auto- and cross-correlation signals. The auto- and cross-correlation signals are obtained by mixing the  $l$  and  $s$

lasers in a potassium dihydrogen phosphate  $\text{KH}_2\text{PO}_4$  [KDP] crystal. The observed autocorrelation signal can be fitted well by the slightly asymmetric exponential function  $f(t) = \exp(\delta\gamma t)$  for  $t \leq 0$  and  $f(t) = \exp(-\gamma t)$  for  $t \geq 0$ . We have set  $\delta = 1.3$ , which is the average value obtained from a set of observed  $I_E(\Delta t)$ . The standard variation between the experimental signal and the convolution of  $f(t)$  with itself is 2.54, which compares favorably with a variation of 8.18 for a Gaussian, or 6.42 for a hyperbolic secant, or 4.14 for a Lorentzian profile. We further assume that the observed broadening of the cross-, compared to the auto-correlation signal can be accounted for by a Gaussian temporal fluctuation (jitter) between the  $l$  and  $s$  lasers. Since the final  $I(\Delta t)$  involves the product of the three fields  $E_l$ ,  $E_s$ ,  $E_p$ , we shift, for convenience, the Gaussian broadening totally on to  $E_s$  and write its temporal profile as

$$f'(t) = [\exp(\delta\gamma t) - (1/z)\exp(z\delta\gamma t)]/(1-1/z)$$

for  $t \leq 0$  and

$$f'(t) = [\exp(-\gamma t) - (1/z)\exp(-z\gamma t)]/(1-1/z)$$

for  $t \geq 0$ . Here, we have taken advantage of the expansion for small values of  $\alpha$  of the Gaussian profile  $\exp(-\alpha t^2)$ . The standard variation between the experimental cross-correlation signal and the convolution of  $f'(t)$  with  $f(t)$  is found to be 1.2 compared to that for the full Gaussian jitter of 0.5. We claim no inherent physical significance for the asymmetric exponential form of  $f(t)$  and  $f'(t)$  or the Gaussian form of the jitter except that they do yield good agreement with data, and that it permits analytical integration of Eq. (1).

Every effort is made before each experimental run to maximize the temporal overlap (at  $\Delta t = 0$ ) between the  $l$  and  $s$  laser. All the same, a temporal mismatch  $\Delta\tau$  of the order of  $\leq 0.5$  ps is often found between the two lasers. (The mismatch can be extracted from the slight asymmetry which it causes in the CARS signal in the vicinity of the peak at  $\Delta t = 0$ .) Finally, the relative contributions of the two components of  $I(\Delta t)$  can be experimentally specified by a quantity  $Y$  defined as the ratio of the peak of the normalized CARS intensity at zero time delay,  $I(\Delta t = 0)$  to the intensity of the phonon dephasing component extrapolated

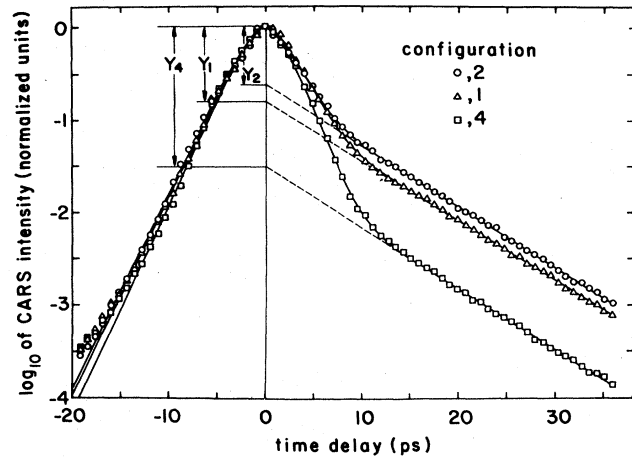


FIG. 1. Experimental data (symbols) and fitted  $I(\Delta t)$  (solid lines) for each of the polarization configurations indicated in the insert to the figure and defined in Table I.

back to  $\Delta t = 0$ . This procedure<sup>5</sup> is illustrated in Fig. 1 for a subset of the laser field polarizations indicated in Table I. [In Table I the polarization direction is given in terms of an angle measured relative to a direction in the plane of the optical table and which is coplanar with the (010) and (100) crystal directions which lie in a plane perpendicular to the optical table.]

At this point, the entire function  $I(\Delta t)$  can be specified (for each polarization condition) in terms of  $Y$ ,  $\Gamma$ ,  $\gamma$ ,  $\delta$ ,  $z$ , and  $\Delta\tau$ . The first two quantities are obtained directly as described above. The remaining quantities (except  $\delta$ ) are determined from a best fit to each  $I(\Delta t)$  as shown by the solid lines in Fig. 1.<sup>6</sup>

It is important to recognize that  $R_a$  and  $\chi^{(3)}$  as they appear in Eqs. (1) and (4) are each effective quantities whose magnitudes depend on the actual polarization (relative to the crystal axes) of the fields  $\vec{E}_l$ ,  $\vec{E}_s$ , and  $\vec{E}_p$ . At resonance the phonon part of  $I(\Delta t)$  is purely imaginary. Moreover,  $\chi^{(3)}$  is in general complex, particularly, in the present case<sup>1</sup> for which  $2\hbar\omega_l$  exceeds the fundamental gap energy, i.e., in

TABLE I. Laser polarization, crystal axis orientation, and effective  $\chi^{(3)}$ .

Configuration	$p$	Polarization condition (deg)			Crystal axis		Effective $\chi^{(3)b}$
		Lasers $l$	$s$	Analyzer <sup>a</sup>	010	100	
1	90	90	180	180	90	180	$\chi_{1221}$
2	90	180	90	180	90	180	$\chi_{1122}$
3	90	90	45	135	45	135	$2\chi_{1122}$
4	90	90	90	90	45	135	$\frac{1}{2}(\chi_{1111} + 2\chi_{1122} + \chi_{1221})$
5	90	90	45	45	45	135	$\chi_{1111} + \chi_{1221}$
6	90	45	90	45	45	135	$\chi_{1111} + \chi_{1122}$
7	90	45	90	135	45	135	$\chi_{1122} + \chi_{1221}$

<sup>a</sup>The analyzer is placed into the CARS beam.

<sup>b</sup>See, e.g., Ref. 1 for an explanation of the subscript convention. The effective  $\chi^{(3)}$  are derived here such that the phonon part of  $I(\Delta t)$  is normalized to unity.

the case that two photon absorptive processes may occur.

The complex effective  $\chi^{(3)}$  for the various polarization conditions are listed in Table I. Note that four out of the seven configurations lead to redundant results. A grand average over 32 runs, distributed over all seven configurations, together with the published value of  $R_a$  for GaP,<sup>7</sup> leads to the following values of the magnitude of the real  $\chi'$  and of imaginary  $\chi''$  parts of the active components of  $\chi^{(3)}$  (in units of  $10^{-10}$  esu):

$$\chi'_{1221} = 2.1 \pm 0.15, \quad \chi''_{1221} = -0.48 \pm 0.24 ;$$

$$\chi'_{1122} = 1.8 \pm 0.44, \quad \chi''_{1122} = -0.7 \pm 0.48 ;$$

$$\chi'_{1111} = 2.1 \pm 0.7, \quad \chi''_{1111} = -0.73 \pm 0.81 .$$

The imaginary part of  $\chi^{(3)}$  has its main effect on  $I(\Delta t)$  through cross terms with the phonon part. For values of  $\chi'' < 10^{-10}$  esu these cross terms effect only slightly the curvature of  $I(\Delta t)$  in the region<sup>2</sup>  $0 < \Delta t < 10$  ps; hence, the relatively large uncertainty in  $\chi''$ . It is observed that the sign of  $\chi''$  is opposite to that of  $\chi'$  and to that of the (positive definite) phonon part.

In order to avoid complications arising from high-lying conduction bands, most previous experimental determinations of  $\chi^{(3)}$ , and most theoretical evaluations<sup>8</sup> have been limited to the "zero frequency limit," i.e., to the case that  $2\hbar\omega_l$  is much less than the gap energy  $E_g$  of the medium so that two-photon absorptive processes can be neglected. This constraint means that  $\chi^{(3)}$  is real, and also leads to the so-called Kleinman symmetry<sup>9</sup> for which  $\chi'_{1122} = \chi'_{1221}$ . This condition is not met in the present experiment of GaP for which  $E_g = 2.26$  eV, whereas  $2\hbar\omega_l = 4.30$  eV. It is, accordingly, not unexpected that we find  $\chi^{(3)}$  to be complex and that  $\chi'_{1122} \neq \chi'_{1221}$ ; the observed ratio  $\chi'_{1221}/\chi'_{1122} = 1.2$ . Moreover, for an isotropic medium we expect the anisotropy factor<sup>1</sup>

$$\sigma = (2\chi'_{1122} + \chi'_{1221} - \chi'_{1111})/\chi'_{1111}$$

to equal zero, whereas 1.7 is observed here. This implies coupling to considerably more anisotropic electronic states than has previously been reported for other tetrahedrally bonded crystals such as diamond<sup>1</sup> ( $\sigma = 0.17$ ), Ge (Ref. 10) ( $\sigma = 0.83$ ), Si (Ref. 10) ( $\sigma = 0.44$ ), and GaAs (Ref. 11) ( $\sigma = 0.56$ ).

Unfortunately, the need to take higher excited electronic bands into account makes it unlikely that the mostly phenomenologically theoretical approaches used so far are applicable to the results reported here.<sup>1</sup> It is particularly unlikely that these models would be able to account for the observed anisotropy in  $\chi^{(3)}$ . On the other hand, it is possi-

ble that the more microscopic, *ab initio*, calculations of semiconductor systems currently being developed<sup>12</sup> will in time become theoretical bases for a comparison to the experimentally observed components of  $\chi^{(3)}$  reported here.

Finally, we make a comparison of the measurements of  $\chi^{(3)}$  in the temporal domain versus those in the spectral domain. It is clear that the two measurements are closely related; the experimental observables being, in effect, Fourier transforms of each other. Nevertheless, differences between the two techniques are discernible. For example, in the spectral domain separate measurements must be performed in order to extract  $\Gamma$  and  $\chi^{(3)}$ , whereas only a single measurement is required in the temporal domain. The determination of  $\chi^{(3)}$  from spectral domain measurements is facilitated if  $\Gamma$  is large (short phonon dephasing time) so that the Raman linewidth is greater than the spectral resolution of the apparatus, whereas best results are obtained in the temporal domain if the phonon dephasing time is larger than the temporal resolution of the apparatus. On the other hand, extraction of  $\chi^{(3)}$  from spectral domain measurements is easiest if the magnitude of the electronic part of  $I(\omega)$  is smaller than the phonon part, whereas the reverse is so for the temporal domain measurements. In the extreme cases only one of the techniques is applicable. For example, the spectral technique must be used if under the experimental conditions  $I_E(\Delta t)$  is much less than the phonon part which was the case of diamond reported in Ref. 1 ( $\chi^3 \sim 10^{-14}$  esu,  $R_a \sim 5$  A<sup>2</sup>),<sup>1</sup> whereas the temporal technique must be used in the opposite limit; e.g., in our case of GaP and particularly ZnSe ( $\chi^{(3)} \sim 10^{-10}$  esu,  $R_a \sim 7$  A<sup>2</sup>).<sup>5</sup> Moreover, we claim a particular advantage for the temporal technique when more than one Raman active resonance appears in the same spectral region. As an example we cite crystals of the zinc-blende structure in which both the TO and LO near-zone-center phonons are active. The superposition of the response from both types of phonons, plus contributions to  $\chi^{(3)}$  from two-step two-wave mixing [ $(\chi^{(2)})^2$ ] makes the analysis of  $I(\omega)$  rather complicated. However, in the temporal technique, when  $\omega_l - \omega_s$  is fixed to the LO phonon resonance and if, in addition,  $2\hbar\omega_p > E_g$  (as it is in the present case), contributions due to the resonance at the TO phonons frequency and to two-wave mixing can be shown to be small.<sup>13</sup> Hence, to a first approximation, only contributions from third-order nonlinear interactions contribute to the  $\chi^{(3)}$  measured here.

We acknowledge the technical assistance of Mr. A. Jonietz and W. Koenig. Two of us (B.K.R. and W.E.B.) further acknowledge financial support through the Army Research Office DAAG 29-83-K-0091.

<sup>1</sup>As an example of the literature in this field, see M. D. Levenson and N. Bloembergen, *Phys. Rev. B* **10**, 4447 (1974).

<sup>2</sup>W. Zinth, A. Laubereau, and W. Kaiser, *Opt. Commun.* **26**, 457 (1978).

<sup>3</sup>J. Kuhl and W. E. Bron, *Solid State Commun.* **49**, 935 (1984).

<sup>4</sup>Some authors refer, alternatively, to this nonlinear interaction as a four-photon-parametric process.

<sup>5</sup>For a preliminary description of the experimental apparatus, see J. Kuhl and D. von der Linde, in *Picosecond Phenomena III*, edited by K. B. Eisenthal, R. M. Hochstrasser, W. Kaiser, and A. Laubereau (Springer-Verlag, Berlin, 1982), pp. 201-204. A more de-

tailed description of the apparatus and of the analysis of the experimental data is to be published at a later time.

<sup>6</sup>The weak nonexponential tail observed in  $I(\Delta t)$  for  $\Delta t \leq -15$  ps can be accounted for by an *ad hoc* weak additional component on the  $t > 0$  side of the temporal profile but which decays at a slower rate than  $\gamma$ . However, the magnitude of this effect is weak (see Fig. 1), and does not interfere with our analysis of  $I(\Delta t)$ .

<sup>7</sup>J. M. Calleja, H. Vogt, and M. Cardona, *Philos. Mag. A* **45**, 239 (1982).

<sup>8</sup>For a review of the theoretical basis, see C. Flytzanis, in *Quantum Electronics: A Treatise*, edited by H. Rabin and C. L. Tang

(Academic, New York, 1978), Vol. 1, pt. A, p. 9.

<sup>9</sup>D. A. Kleinman, Phys. Rev. **126**, 1977 (1962).

<sup>10</sup>J. J. Wynne, Phys. Rev. **178**, 1295 (1969).

<sup>11</sup>E. Yablonovitch, C. Flytzanis, and N. Bloembergen, Phys. Rev. Lett. **29**, 865 (1972).

<sup>12</sup>See R. M. Martin, J. Phys. (Paris) Colloq. **42**, C6-617 (1981), and references cited therein.

<sup>13</sup>See, for example, C. Flytzanis and N. Bloembergen, Prog. Quantum Electron. **4**, 271 (1976). The terms in  $\chi_{xyzE}^{(2)}$  in Eq. (2.77) of

this reference vanish or are negligibly small either (i) because no electromagnetic field propagates in the medium when  $\Delta\omega = \omega_l - \omega_s = \omega_{LO}$  since  $\epsilon(\omega_{LO}) = 0$ , or (ii) because in our experiment  $2\hbar\omega_l > E_g$  so that the corresponding terms in (2.77) are of the order of  $[4\pi(\chi_{xyzE}^{(2)})^2/\epsilon(2\omega_l)]/3\chi^{(3)} \approx 10^{-2}$ . [See, for example, R. A. Soref and H. W. Moos, J. Appl. Phys. **35**, 2152 (1964).] The last term in (2.77) is also small since  $\Delta\omega \neq \omega_{TO}$ .